Structural and Electronic Properties of Stable Au_nIr_2 ($n = 1-7$) Clusters: Comparison with Pure Gold Clusters

Li-Ping Ding[a], Xiao-Yu Kuang[a,b], Peng Shao[a], Ming-Min Zhong[a], and Yan-Fang Li[a]

[a] Institute of Atomic and Molecular Physics, Sichuan University, Chengdu 610065, China
[b] International Centre for Materials Physics, Academia Sinica, Shenyang 110016, China

Reprint requests to X. K.; E-mail: scu_kuang@163.com

Z. Naturforsch. **67a,** 729 – 738 (2012) / DOI: 10.5560/ZNA.2012-0086
Received January 18, 2012 / revised September 9, 2012 / published online November 14, 2012

The geometrical structures, relative stabilities, electronic and magnetic properties of Au_nIr_2 ($n = 1-7$) clusters have been systematically investigated by using meta-generalized gradient approximation (meta-GGA) Tao–Perdew–Staroverov–Scuseria (TPSS) functional in comparison with pure gold clusters. The optimized geometries show that the two doping iridium atoms can affect the structure of the host cluster. Compared with the pure Au_{n+2} clusters, the lowest energy Au_nIr_2 ($n = 1-7$) clusters favour higher spin multiplicity except for Au_7Ir_2. Furthermore, the calculated binding energies, fragmentation energies, second-order difference energies, and the highest occupied–lowest unoccupied energy gaps indicate that the stability of Au_nIr_2 is enhanced. Natural population analysis reveals that the charges transfer from the Au_n frames to the iridium atoms for $Au_{3,4,6,7}Ir_2$ clusters. In addition, charges and magnetic moments of 6s, 5d, and 6p states for the iridium atoms in Au_nIr_2 ($n = 1-7$) clusters are also analyzed and compared.

Key words: Meta-GGA Exchange Correlation Functional (TPSS); Au_nIr_2 ($n = 1-7$) Clusters; Geometric Structure.

1. Introduction

Clusters are a group of atoms that come together and whose physical and chemical properties change with the increasing number of atoms. They can be comprised of anywhere between a few and tens of thousands of atoms and represent a sort of bridge between the atomic and bulk size regimes. In recent years, much of the interest in gold and doped gold clusters is fuelled by their special applications in the fields of catalysis, surface science, microelectronics, and optical materials [1 – 11]. Especially, because transition metal atoms possess unfilled d orbitals, their electronic structure and chemical properties depend upon the interplay between s and d electrons and can strongly change the properties of the host cluster [12 – 18]. Transition metal atoms doped in gold clusters have been a common topic of great interest for experimental and theoretical investigation on their structural and electronic properties.

For instance, Bouwen et al. [19] investigated the bimetallic $Au_nX_m{}^+$ (X = Cu, Al, Y, and In; $n = 1-65, m = 1,2$) clusters by a dual-target dual-laser vapourization source and studied their stabilities using time-of-flight mass abundance spectrometry. They found that $Au_nCu_m{}^+$ clusters exhibit the same electronic shell effects as $Au_n{}^+$, and Au_nAl^+ have different abundance patterns compared to Au_nY^+ or Au_nIn^+. Janssens et al. [20], using cationic photofragmentation mass spectrometry, investigated Au_5X^+ (X = V, Mn, Cr, Fe, Co, Zn) clusters and found strongly enhanced stabilities. Yuan et al. [21] investigated the geometric, electronic, and bonding properties of Au_nM ($n = 1-7, M$ = Ni, Pd and Pt) clusters and found that the doped atoms markedly changed the geometric and electronic properties of gold clusters. Tanaka et al. [22] have been predicted that all of the lowest energy isomers of Au_nZn ($n \leq 6$) clusters and their cations are 2D structures by density functional theory (DFT). The geometric and electronic properties of doped Au_nY ($n = 1-9$) clusters are investigated by Mao et al. [23]. In previous works, the structure and bonding of $Au_nSi_2^-$ and Au_nSi_2 ($n = 2,4$) clusters are reported by Li et al. [24], they found that the dibridged and monobridged structure are the most stable structures of Au_2Si_2 and Au_4Si_2 clusters, respectively. Recently, Guo et al. studied the structures and stabilities of Au_nPt_2 ($n = 1-4$) clusters [25], and their results in-

Table 1. Calculated bond lengths r [Å], dissociation D_e [eV], and frequencies ω_e [cm^{-1}] for the lowest energy Ir_2, Au_2, and AuIr clusters in quintet, singlet, and triplet state, respectively.

Clusters	Ir_2			Au_2			AuIr		
Method/basis set	r	D_e	ω_e	r	D_e	ω_e	r	D_e	ω_e
B3LYP/LANL2DZ	2.26	3.02	285	2.57	1.87	162	2.55	2.03	171
BP86/LANL2DZ	2.27	4.34	280	2.55	2.15	168	2.52	2.33	182
PW91PW91/LANL2DZ	2.26	5.61	281	2.55	2.20	169	2.52	2.98	182
TPSSTPSS/LANL2DZ	2.26	4.00	285	2.54	2.19	174	2.51	2.33	185
B3LYP/SDD	2.27	3.92	281	2.58	1.86	163	2.57	2.00	173
BP86/SDD	2.27	5.03	276	2.56	2.14	168	2.52	2.66	179
PW91PW91/SDD	2.27	4.25	277	2.56	2.19	167	2.52	2.34	179
TPSSTPSS/SDD	2.26	3.80	280	2.55	2.15	171	2.52	2.26	182
B3LYP/CEP-121G	2.30	2.56	269	2.57	1.90	165	2.55	2.01	170
BP86/CEP-121G	2.27	5.47	275	2.55	2.19	170	2.55	2.97	181
PW91PW91/CEP-121G	2.27	5.12	275	2.55	2.25	170	2.52	2.83	181
TPSSTPSS/CEP-121G	**2.27**	**3.77**	**279**	**2.53**	**2.21**	**174**	**2.51**	**2.29**	**183**
Experimental	**2.35**[a]	**3.46±0.12**[d]	**280**[a]	**2.47**[b]	**2.29**[b]	**191**[b]	**2.55**[c]	**2.27**[c]	**169**[c]

[a,d][40],[42] [b][41] [c][15]

dicated that the gold-doped atoms interaction is strong enough to enhance the cluster stability, and the larger the Au_n cluster, the smaller the distortions caused by the two Pb or Pt atoms. In comparison with other transition metals, few is known about the single iridium doped gold cluster. Only Yang et al. [26] performed the investigation on Au_nIr $(n = 1-8)$ clusters, and they found that all ground states possess planar structures expect for $n = 7$. But the transition metal iridium atom plays an important role in catalysis [27–29], and the studies on iridium as catalyst have little theories and reactivity experiments [30–36]. In addition, we are interested in what does change as the two iridium atoms dope; whether more 3D structures occur or not; are there different properties from pure gold? Thus, we studied the Au_nIr_2 clusters in this paper to provide more databases for experimental and theoretical investigation in the future.

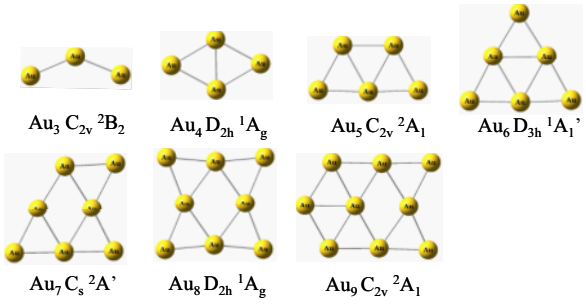

Fig. 1 (colour online). Lowest energy structures of pure gold clusters for each size. The corresponding point-group symmetries and electronic states are also given.

In the present paper, we systematically investigate the geometric structures and stability trend of Au_nIr_2 $(n = 1-7)$ clusters by the meta-generalized gradient approximation (meta-GGA) Tao-Perdew-Staroverov-Scuseria (TPSS) functional [37] including the kinetic energy density in the functional expression. The motivation of our work is threefold. Our first intention is to give an exploratory study of the geometric structures and growth pattern for Au_nIr_2 $(n = 1-7)$ clusters. Secondly, it is to probe the different electronic properties of the bimetallic clusters that effect by doped atoms; furthermore, some interesting changes are compared in series alloy and bare clusters. We are motivated, thirdly, by the hope that such a study might offer relevant information for further experimental and theoretical studies.

2. Computational Details

As the meta-generalized gradient approximation (meta-GGA) functional includes the kinetic energy density in the functional expression, the more accurate results both for the atomization energy and the relative stability are produced. So in our calculations, the meta-GGA Tao–Perdew–Staroverov–Scuseria (TPSS) functional was used to instead of the traditional GGA functional. All optimizations of the Au_{n+2} and Au_nIr_2 $(n = 1-7)$ clusters were performed by the GAUSSIAN03 program [38] with the TPSS functional and CEP-121G basis set. The CEP-121G basis set was derived from numerical Dirac–Fock atomic wavefunctions using shape-consistent valence pseudo-orbitals

and an optimizing procedure based on an energy-overlap functional [39]. In search for the lowest energy structure, lots of possible initial structures, which include one-, two- and three-dimensional configurations, have been considered in geometry optimizations and all the clusters are relaxed fully without any symmetry constraints. Furthermore, every initial configuration was optimized at various possible spin multiplicities due to the spin polarization and each of them was analyzed by harmonic vibrational frequencies to confirm that we obtained the local minimum geometry. In order to check the intrinsic reliability and accuracy of the computational method, we chose Au_2, Ir_2, and AuIr dimers as examples to calculate bond lengths, vibration frequencies, and dissociation energies by using different method and basis set. The calculated results are compared with the available experimental values [15, 40–42] and listed in Table 1. On the whole, among lots of the available methods, the TPSSTPSS/CEP-121G gives the best estimate. And the TPSSTPSS/CEP-121G level of theory gives 0.9% (AuIr) and 7.7% (Ir_2) error in dissociation energy and 3.6% (Ir_2) error in vibrational frequency which is still better than some of the theoretical values 6.2% (AuIr) and 10.9% (Ir_2) error in dissociation energy and 11.4% (Ir_2) error in vibrational frequency reported earlier [27]. In addition, the bond length and frequency for the Ir_2 dimer are fitting well with the results of Jules and Lombardi (R = 2.23 Å and $\omega_e = 280$) [43], Du and Yuan (R = 2.27 Å and $\omega_e = 278$) [44], and the experimental values. The dissociation energy (3.50 eV) is also in excellent agreement with the experimental values.

3. Result and Discussion

3.1. Geometries

3.1.1. Bare Gold Clusters Au_{n+2} $(n = 1-7)$

In order to discuss the effects of impurity atoms on gold clusters, some optimizations, calculations, and discussions on pure gold clusters Au_{n+2} $(n = 1-7)$ first were performed referencing previous works [45–49] by using the meta-GGA TPSS functional method. The results of optimization indicate that all the ground states are in line with those extracted from the literature. The ground states of gold clusters for each size are shown in Figure 1.

Table 2. Spin multiplicity, symmetries, electronic states, relative energies ΔE [eV] of Au_nIr_2 $(n = 1-7)$ clusters.

isomers	multiplicity	symmetry	state	ΔE
1a	6	C_s	$^6A'$	0.00
1b	8	C_s	$^8A'$	0.79
1c	6	C_{2v}	$^6A_2$	1.71
1d	8	C_{2v}	$^8B_1$	3.10
2a	5	C_s	$^5A''$	0.00
2b	5	D_{2h}	$^5B_{2g}$	0.05
2c	5	C_s	$^5A'$	0.08
2d	7	C_s	$^7A'$	0.35
2e	7	C_{2v}	$^7A_2$	0.38
2f	5	C_{2v}	$^5A_1$	0.57
2g	1	C_s	$^1A'$	1.90
3a	4	C_{2v}	$^4A_2$	0.00
3b	6	C_s	$^6A''$	0.11
3c	6	C_1	^6A	0.14
3d	4	C_{2v}	$^4A_2$	0.38
3e	6	C_s	$^6A''$	0.44
3f	6	C_{2v}	$^6B_1$	0.71
3g	8	C_1	^8A	0.93
4a	5	C_{2v}	$^5B_1$	0.00
4b	5	C_s	$^5A'$	0.35
4c	5	C_s	$^5A''$	0.44
4d	7	C_s	$^7A'$	0.87
4e	5	C_s	$^5A'$	1.01
4f	5	C_{2v}	$^5B_2$	1.36
4g	5	C_{2v}	$^5A_1$	1.93
5a	4	C_s	$^4A''$	0.00
5b	4	C_s	$^4A''$	0.30
5c	2	C_s	$^2A''$	0.44
5d	6	C_s	$^6A'$	0.71
5e	2	C_1	^2A	0.93
5f	4	C_1	^4A	1.06
5g	6	C_s	$^6A''$	2.15
6a	5	C_1	^5A	0.00
6b	5	C_s	$^5A'$	0.08
6c	1	C_{2v}	$^1B_2$	0.27
6d	5	C_s	$^5A''$	0.49
6e	5	C_s	$^5A'$	0.73
6f	5	D_2	$^5B_1$	1.01
6g	7	C_s	$^7A'$	1.33
7a	2	C_{2v}	$^2B_1$	0.00
7b	4	C_s	$^4A''$	0.16
7c	4	C_{2v}	$^4A_2$	0.60
7d	4	C_s	$^4A''$	1.06
7e	4	C_s	$^4A''$	1.09
7f	6	C_{2v}	$^6A_1$	1.93
7g	2	C_s	$^2A''$	2.83

3.1.2. Bimetallic Iridium–Gold Clusters Au_nIr_2 $(n = 1-7)$

To search for the lowest energy structures of Au_nIr_2 $(n = 1-7)$ clusters, we search them by placing two iridium atoms at various adsorption or substitu-

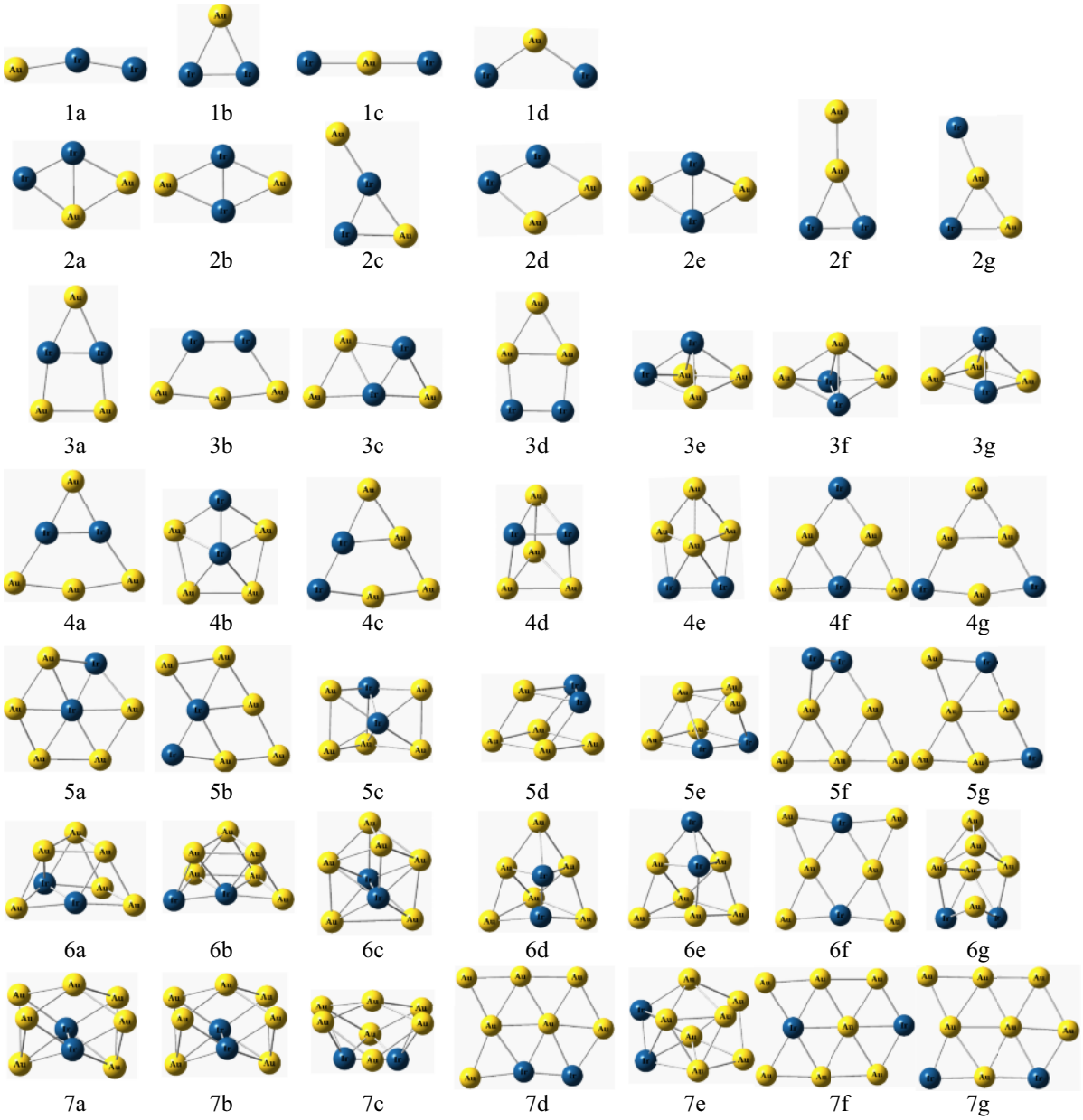

Fig. 2 (colour online). Lowest energy structure and a few low-lying isomers for doped clusters.

tion sites on the basis of optimized Au_{n+2} $(n = 1-7)$ clusters geometries, i.e., iridium-capped, iridium-substituted, and iridium-concaved patterns, as well as gold-capped pattern. A large number of optimized isomers for Au_nIr_2 $(n = 1-7)$ clusters are obtained and the low-lying isomers for each size are only selected and listed in Figure 2. According to the total energies from low to high, these isomers are designated by *n*a, *n*b, *n*c, *n*d, *n*e, *n*f, and *n*g ('*n*' is the number of gold atoms in the Au_nIr_2 clusters). Meanwhile, their spin multiplicity, symmetry, electronic state, and energy differences compared to each of the lowest energy isomers are presented in Table 2.

The lowest energy structure of $AuIr_2$ (1a) is a sextet with C_s point symmetry, and its Au–Ir–Ir apex angle is 162°, in which the two iridium atoms located at the same side. It is energetically lower than the other two triangle structures with octet spin multiplicity (1b of 0.79 and 1d of 3.10 eV). All possible initial structures of Au_2Ir_2 clusters with different spin multiplicities were optimized. The calculated results illustrate that the lowest energy isomer (2a) is a planar quadrilateral structure with 7.71 eV vertical ionization energy (VIP), and the corresponding electronic state is a quintet state $^5A''$. In addition, we found that y-shaped and Y-shaped isomers with two iridium atoms substituting different sites of the Au_4 host are less favourable in energy. With regard to the Au_3Ir_2 cluster, the most stable structure 3a and the other two different low-lying isomers 3b and 3c are obtained within an energy range of 0.08 eV. The lowest energy structure 3a, with symmetry C_{2v} and quartet state $^4A_2$, is the planar house-like. The geometry of the 3b isomer was found to be trapezoid with an Ir–Ir distance of 2.36 Å longer than that of the lowest energy isomer 3a (2.29 Å). This longer Ir–Ir distance suggests the reduced stability of isomer 3b relative to 3a. At $n = 4$, the distorted triangle structure 4a can be viewed as one substituted-isomer of the ground state Au_6, which has C_{2v} symmetry and a $^5B_1$ electronic state. Another three isomers (4c, 4f, and 4g), which have the similar structure as the 4a isomer, are higher 0.24, 1.20, and 1.85 eV in total energy than the lowest energy isomer, respectively. For Au_5Ir_2 clusters, the most stable isomer 5a with C_s symmetry is generated by capping the 4b structure with one gold atom; its VIP value is 7.16 eV. The isomers 5b, 5d, 5e, and 5g are four structures derived from the low-lying isomers of the Au_4Ir_2 cluster, where the fifth gold atom added to the Au_4Ir_2 clusters in different sites. From $n = 5$ afterwards, the three-dimensional structures show higher stability than the planar clusters. For Au_6Ir_2 clusters, a lot of possible structural configurations and spin states are considered to identify the ground state. The optimized results show that isomers 6a, 6b, 6d, 6e, and 6g can be viewed as two gold atoms of the ground state Au_8 cluster are substituted by two iridium atoms. The 3D structure 6a with ^5A electronic state is the most stable structure among the investigated isomers. In the case of Au_7Ir_2, the lowest energy structure of Au_7Ir with C_{2v} symmetry is marked by two iridium atoms substituting two gold atoms in the Au_9 cluster. It is interesting to find that the 3D structure (7a, 7b, 7c, and 7e) occur when two iridium atoms replace gold atoms of the planar ground state Au_9 cluster in different directions. As we can see from Figure 2, the obtained isomers by iridium atoms bonding directly are more favourable in energy than other situations, which may be related to the smaller atomic radius of the iridium atom, and the Au–Ir bond-

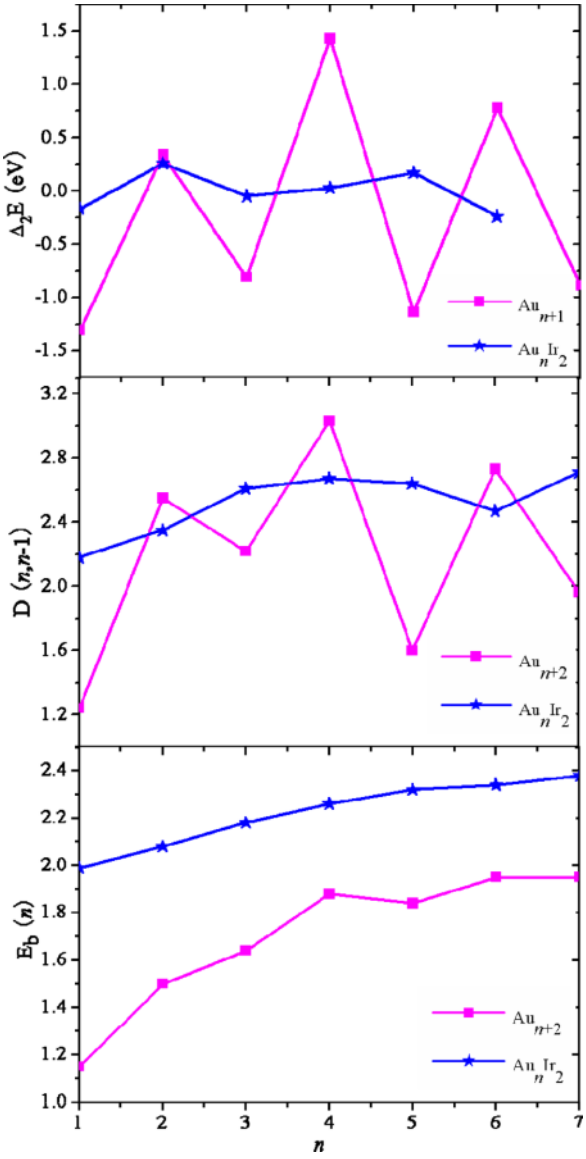

Fig. 3 (colour online). Size dependence of the averaged atomic binding energies, the fragmentation energies, and the second-order difference of energies for the most stable Au_nIr_2 $(n = 1-7)$ and Au_{n+2} $(n = 1-7)$ clusters.

ing contain the d-electron contributions of the iridium atom.

Compared with the optimized lowest energy Au_{n+2} $(n = 1-7)$ structures, we can find that the lowest energy geometries of Au_nIr_2 $(n = 1-7)$ clusters in our discussion appear as 3D structure at $n = 6$ and 7. This indicates the transition point of the 2D structure to 3D for doped cluster has been shifted to an earlier size, and these structures favour higher spin multiplicity except for Au_7Ir_2. The two iridium atoms in the ground state Au_nIr_2 $(n = 1-7)$ clusters tend to form a bond with each other directly, and Ir_2 is always intact in most of the lowest energy clusters. In addition, the Au_{n+2} clusters structure substituted by two iridium atoms is the dominant growth pattern for Au_nIr_2 clusters of various sizes.

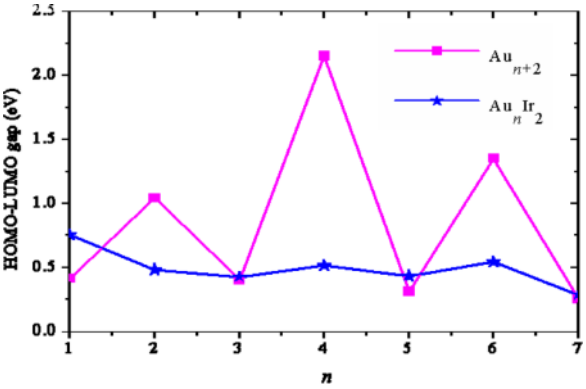

Fig. 4 (colour online). Size dependence of the HOMO–LUMO gap for the lowest energy structures of Au_nIr_2 $(n = 1-7)$ clusters.

3.2. Relative Stabilities

To gain insight into the stability of Au_nIr_2 $(n = 1-7)$ clusters, the binding energy per atom E_b, fragmentation energy D, and the second-order difference energy Δ_2E are calculated. They can be expressed as

$$E_b(n) = [2E(\mathrm{Ir}) + nE(\mathrm{Au}) - E(\mathrm{Au}_n\mathrm{Ir}_2)]/(n+2), \quad (1)$$

$$D(n, n-1) = E(\mathrm{Au}_{n-1}\mathrm{Ir}_2) + E(\mathrm{Au}) - E(\mathrm{Au}_n\mathrm{Ir}_2), \quad (2)$$

$$\Delta_2E(n) = E(\mathrm{Au}_{n-1}\mathrm{Ir}_2) + E(\mathrm{Au}_{n+1}\mathrm{Ir}_2) - 2E(\mathrm{Au}_n\mathrm{Ir}_2), \quad (3)$$

where $E(\mathrm{Au}_{n-1}\mathrm{Ir}_2)$, $E(\mathrm{Au})$, $E(\mathrm{Ir})$, $E(\mathrm{Au}_n\mathrm{Ir}_2)$, and $E(\mathrm{Au}_{n+1}\mathrm{Ir}_2)$, respectively, denote the zero point energy (ZPE) corrected energies of the $Au_{n-1}Ir_2$, Au, Ir, Au_nIr_2, and $Au_{n+1}Ir_2$ clusters.

Considering the influence of the impurity atom on small pure clusters, E_b, D, and Δ_2E for pure Au_{n+2} clusters are also studied using the following formulae:

$$E_b(n+2) = [(n+2)E(\mathrm{Au}) - E(\mathrm{Au}_{n+2})]/(n+2), \quad (4)$$

$$D(n+2, n+1) = E(\mathrm{Au}_{n+1}) + E(\mathrm{Au}) - E(\mathrm{Au}_{n+2}), \quad (5)$$

$$\Delta_2E(n+2) = E(\mathrm{Au}_{n+1}) + E(\mathrm{Au}_{n+3}) - 2E(\mathrm{Au}_{n+2}), \quad (6)$$

where $E(\mathrm{Au})$, $E(\mathrm{Au}_{n+1})$, $E(\mathrm{Au}_{n+2})$, and $E(\mathrm{Au}_{n+3})$ represent the total energies of the lowest energy clusters or atoms for the Au, Au_{n+1}, Au_{n+2}, Au_{n+3} clusters, respectively.

The E_b, D, and Δ_2E values of the Au_{n+2} and Au_nIr_2 clusters at TPSSTPSS/CEP-121G level of theory as a function of clusters size are plotted in Figure 3. The figure show some interesting results as following.

(i) The atomic average binding energy of Au_nIr_2 doped counterparts is obviously larger than that of the corresponding pure gold cluster. With size of clusters increasing, the binding energy of pure gold cluster increases gradually and reaches the maximum value of 1.95 eV. Meanwhile, the binding energy of Au_nIr_2 cluster also increases gradually and reaches the maximum value of 2.38 eV. This indicates that the Au_nIr_2 cluster is more stable than the corresponding pure gold cluster energetically and reflects that the stability of the Au_nIr_2 cluster is enhanced when two iridium atoms are doped in the pure Au_{n+2} clusters.

(ii) The fragmentation energy of pure Au_{n+2} clusters show an obvious odd–even oscillations, indicating that even-numbered gold clusters are relatively more stable than the neighbouring odd-numbered size. For the doping impurity atom clusters, the curve increase smoothly from 1 to 3, after that, it shows a weak oscillation. It is more interesting to note that the values of fragmentation energies for doped Au_nIr_2 clusters at $n = 3$, 4, and 5 are almost unchanged, while it reaches the minimum value of 2.47 eV at $n = 6$.

(iii) The second-order difference energy curve shows that the Au_2Ir_2 and Au_5Ir_2 clusters have the largest Δ_2E value of 0.26 and 0.17 eV/atom, respectively. So, it can be deduced that they possess relatively high stability.

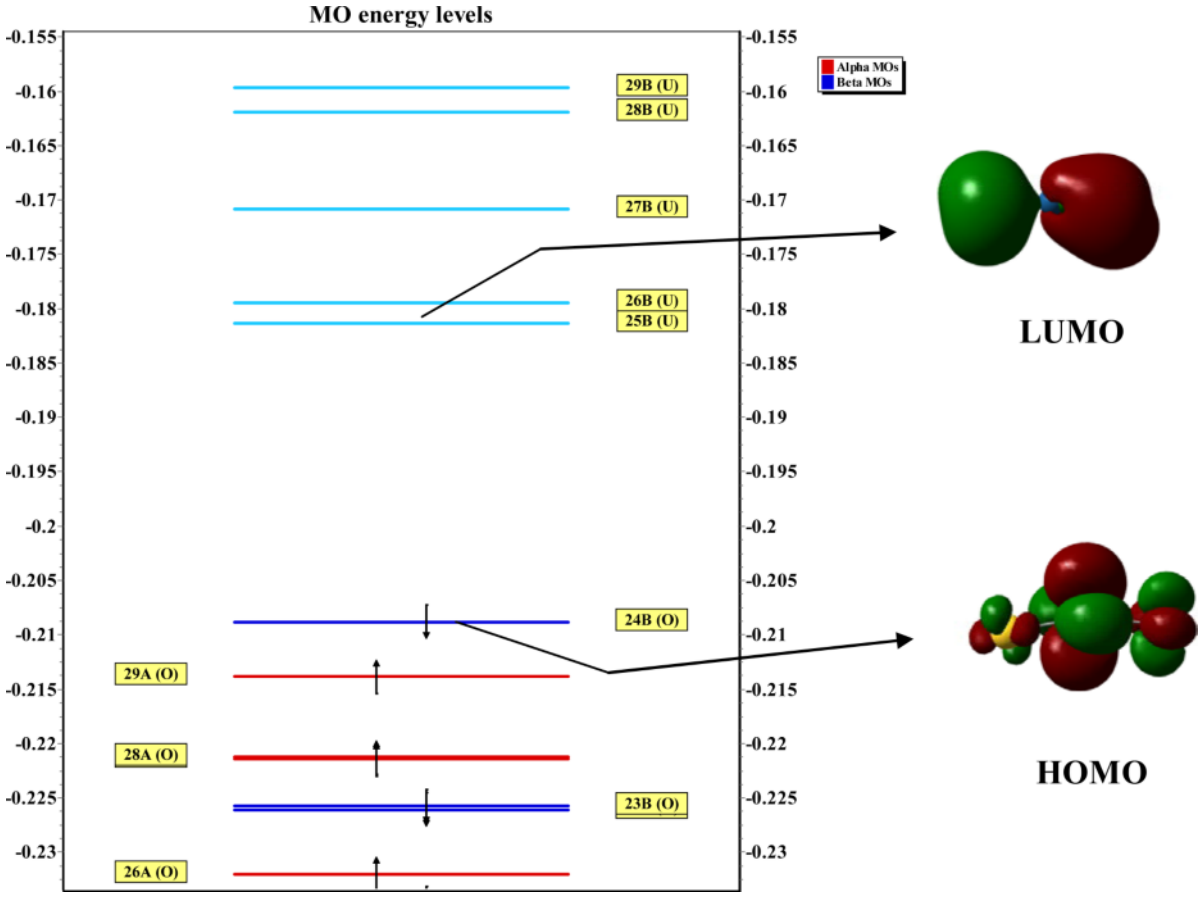

Fig. 5 (colour online). Calculated molecular orbital energy level of $AuIr_2$ together with a molecular orbital map for the HOMO and LUMO; the isovalue is 0.02 a.u.

3.3. Electronic Properties

The highest occupied–lowest unoccupied molecular orbital (HOMO–LUMO) energy gap reflects the ability of electrons to jump from an occupied orbital to an unoccupied orbital, and represents the ability for the molecule to participate in the chemical reactions to some degree. A large gap corresponds to higher stability, namely a large gap indicates a weaker chemical activity. The HOMO–LUMO energy gaps for the most stable geometry on pure Au_{n+2} and doped Au_nIr_2 $(n = 1-7)$ clusters are plotted against the cluster size in Figure 4. As seen from the plot, the curve of pure gold clusters show obvious odd–even oscillations. The electron pairing effect can explain the oscillatory trends. The odd- (even-) sized clusters have an odd (even) total number of valence electrons and the HOMO is singly (doubly) occupied. The electrons in a doubly occupied HOMO have stronger effective core potentials because the electron screening is weaker for electrons in the same orbital than for inner shell electrons. The clusters can more easily acquire an electron in the open-shell HOMO of the system with odd-numbered electrons than in the LUMO of a closed-shell system. The curve of Au_nIr_2 clusters decrease smoothly at $n = 1-3$; afterward, as the size is increasing, the curve has very slightly odd–even oscillations. Additionally, the values of $n = 3, 5,$ and 7 almost equal to that of $Au_{3,5,7}$ clusters. This may be due to the fact that the two doped iridium atoms have little effect on the electronic structure of pure gold clusters. Meanwhile, the $AuIr_2$ cluster has the larger HOMO–LUMO gap (0.75 eV) compared with other clusters, indicating that the $AuIr_2$ is more stable than its neighbouring clusters.

Table 3. Natural populations analysis (NPA) of the lowest energy Au_nIr_2 $(n = 1-7)$ clusters.

n	Ir-1	Ir-2	Au-3	Au-4	Au-5	Au-6	Au-7	Au-8	Au-9
1	0.06406	0.05987	−0.12393						
2	−0.02158	−0.06905	0.15441	−0.06377					
3	−0.06209	−0.06209	0.03328	0.03328	0.05762				
4	−0.18887	−0.18887	0.04487	0.09144	0.14999	0.09144			
5	0.09520	−1.00028	0.11929	0.20494	0.20494	0.18795	0.18795		
6	−0.28491	−0.69872	0.14634	0.07869	0.25725	0.13545	0.15504	0.21087	
7	−0.82658	−0.82658	0.25009	0.31911	0.25009	0.25009	0.01458	0.25009	0.31911

In order to investigate the $AuIr_2$ cluster, the molecular orbital energy levels and contour maps for the HOMO and LUMO are displayed in Figure 5. The overlap between the frontier orbitals is illustrated. Meanwhile, the HOMO involves the 1s and $6d_z$ orbitals from the gold atom and the 1s and $3p_x$ orbitals from the iridium atoms; the LUMO mostly involves the $3p_z$ and $5d_{xz}$ orbitals of the gold atom as well as the $1p_z$ and $5d_{yz}$ orbitals of the iridium atoms. These molecular orbitals indicate that spd hybridization occurs between the gold and iridium atoms.

Our natural population analysis (NPA) can provide reliable charge-transfer (CT) information [50], and the results for the lowest energy Au_nIr_2 species are summarized in Table 3. NPA clearly shows the ionic character of the Au–Ir bond in these clusters. The iridium atoms of Au_3Ir_2, Au_4Ir_2, Au_6Ir_2, and Au_7Ir_2 clusters possess charges in the range of -0.06209 to -1.00028 electrons, indicating that the charges in these cluster transfers from the Au_n frame to iridium atoms. The two iridium atoms derive equal electrons in the Au_nIr_2 clusters when $n = 3,4,7$. From Figure 2, we can see that the two iridium atoms in Au_3Ir_2, Au_4Ir_2, and Au_7Ir_2 almost lie in the same position. This may suggest that the charge distribution is dependent on the symmetry of the cluster. While the charges transfer from iridium atoms to the Au_n frame for the $AuIr_2$ cluster, so the Au_n behaves as a charge acceptor. According to the above discussion, the results may be related with the fact that there is almost no different electronegativity between iridium (2.20) and gold (2.54).

3.4. Magnetic Properties

To further understand the electronic and magnetic properties of Au_nIr_2 $(n = 1-7)$ clusters, we performed a systematically analysis of the onsite atomic internal charge transfer and local magnetic moments for the lowest energy structure of Au_nIr_2 clusters. The charges and magnetic moments of 6s, 5d, and 6p states for the two iridium atoms in Au_nIr_2 clusters are summarized in Table 4. For a free iridium atom, the configuration of valence electrons is $5d^76s^2$. By comparing with this configuration, we can find that the 6s state loses $0.64-1.36$ electrons, and the 5d and 6p states gain some amount of electrons. In addition, by comparing the configuration of valence electrons ($5d^{10}6s^1$) of isolate gold atoms with the natural electron configurations (Au: $6s^{1.38}5d^{9.74}6p^{0.01}$) in the doped $AuIr_2$ cluster,

Table 4. Charge and magnetic moment of 6s, 5d, and 6p states for the iridium atoms in Au_nIr_2 $(n = 1-7)$ clusters.

		Isomers	$AuIr_2$	Au_2Ir_2	Au_3Ir_2	Au_4Ir_2	Au_5Ir_2	Au_6Ir_2	Au_7Ir_2
Ir (1)	6s	Q (e)	1.36	0.80	0.87	0.83	0.78	0.64	0.65
		$\mu(\mu_B)$	0.16	0.06	0.07	0.10	0.07	0.01	0.02
	5d	Q (e)	7.56	7.95	7.86	7.98	7.98	8.15	8.27
		$\mu(\mu_B)$	2.30	1.87	1.40	1.82	1.72	0.02	0.51
	6p	Q (e)	0.03	0.26	0.32	0.37	0.14	0.49	0.90
		$\mu(\mu_B)$	0	0.02	0	0.01	0	0.03	0
Ir (2)	6s	Q (e)	1.17	1.11	0.87	0.83	0.73	0.67	0.65
		$\mu(\mu_B)$	0.11	0.19	0.07	0.10	0.02	0.09	0.02
	5d	Q (e)	7.52	7.88	7.86	7.98	8.28	8.17	8.27
		$\mu(\mu_B)$	2.30	1.78	1.40	1.82	1.59	1.59	0.51
	6p	Q (e)	0.24	0.08	0.32	0.37	0.96	0.84	0.90
		$\mu(\mu_B)$	−0.02	0	0	0.01	0	0.04	0

we noted when gold bond to Ir_2, the single gold atom (6s) also gain some amount of electrons. So exists spd hybridization in iridium atoms and strong hybridization between two iridium atoms and gold atoms. The magnetic moments of the iridium atoms are mainly located on the 5d state, only little of them come from 6s and 6p states; the distribution of magnetic moments on the two iridium atoms is almost equal in identical clusters.

4. Conclusions

Using the meta-GGA TPSS functional and CEP-121G basis set, we investigated the geometrical structures, relative stabilities, and electronic and magnetic properties of iridium-doped gold clusters Au_nIr_2 $(n = 1-7)$ systematically, combined with pure gold clusters for comparison. Several interesting results are summarized as follows:

(i) The calculated results revealed that all the lowest energy geometries of Au_nIr_2 $(n = 1-7)$ clusters may be generated mainly by substituting two gold atoms of the Au_{n+2} cluster with iridium atoms. The most stable Au_nIr_2 $(n = 1-7)$ clusters geometry appears as 3D structure at $n = 6$ and 7. Comparing with corresponding pure Au_{n+2} clusters, the transition point of the 2D structure to 3D has been shifted to an earlier size, and these structures favour higher spin multiplicity except for Au_7Ir_2.

(ii) The average atomic binding energies indicate that the stability of Au_nIr_2 is enhanced dramatically when two iridium atoms are doped in the pure Au_{n+2} clusters. The curves of the fragmentation energy and second-order difference energy show weak odd–even oscillation. The HOMO–LUMO gaps exhibit that the even-numbered Au_nIr_2 clusters are relatively more stable than the vicinity clusters expect for Au_2Ir_2.

(iii) the NPA analysis reveals that the charges transfer from the Au_n frame to iridium atoms for the Au_3Ir_2, Au_4Ir_2, Au_6Ir_2, and Au_7Ir_2 clusters, and the two iridium atoms derive equal electrons expect for Au_6Ir_2. The magnetic moment induced on the surrounding gold atoms is very small, and most of the contribution to the magnetic moment of the clusters comes from the iridium atoms.

Acknowledgement

The authors are grateful to the National Natural Science Foundation of China (No. 10974138 and No. 11104190) and the Doctoral Education Fund of Education Ministry of China (No. 20100181110086 and No. 20110181120112).

[1] G. Bravo-Pérez, I. L. Garzón, and O. Novaro, J. Mol. Struct. (Theochem.) **493**, 225 (1999).
[2] G. Bravo-Pérez, I. L. Garzón, and O. Novaro, Chem. Phys. Lett. **313**, 655 (1999).
[3] K. J. Taylor, C. L. Pettiette-Hall, O. Cheshnovsky, and R. E. Smalley, J. Chem. Phys. **96**, 3319 (1992).
[4] M. A. Cheeseman and J. R. Eyler, J. Phys. Chem. **96**, 1082 (1992).
[5] S. F. L. Mertens, C. Vollmer, A. Held, M. L. Aguirre, M. Walter, C. Janiak, and T. Wandowskil, Angew. Chem. Int. Ed. **50**, 9735 (2011).
[6] E. Redel, M. Walter, R. Thomann, L. Hussein, M. Kruger, and C. Janiak, Chem. Commun. **46**, 1159 (2010).
[7] E. Redel, M. Walter, R. Thomann, C. Vollmer, L. Hussein, H. Scherer, M. Kruger, and C. Janiak, Chem. Eur. J. **15**, 10047 (2009).
[8] E. M. Femández, J. M. Soler; I. L. Garzón, and L. C. Balbás, Condens. Matter Phys., Phys. Rev. B **70**, 165403 (2004).
[9] B. M. Quinn, C. Dekker, and S. G. Lemmay, J. Am. Chem. Soc. **127**, 6146 (2005).
[10] E. Cottancin, G. Celep, J. Lermé, M. Pellarin, J. R. Huntzinger, J. L. Valle, and M. Broyer, Theor. Chem. Acc. **116**, 514 (2006).
[11] R. Fournier, J. Chem. Phys. **115**, 2165 (2001).
[12] D. Die, X. Y. Kuang, J. J. Guo, and B. X. Zheng, J. Mol. Struct. (Theochem.) **902**, 54 (2009).
[13] C. Mihut, C. Descorme, D. Duprez, and M. D. Amiridis, J. Catal. **212**, 125 (2002).
[14] F. Hao, Y. Zhao, X. Li, F. Liu, J. Mol. Struct. **807**, 153 (2007).
[15] Z. J. Wu, Chem. Phys. Lett. **406**, 24 (2005).
[16] K. Koyasu, Y. Naono, M. Akutsu, M. Akutsu, M. Mitsui, and A. Nakajima, Chem. Phys. Lett. **422**, 62 (2006).
[17] B. K. Vlasta, B. Jaroslav, M. Roland, M. Ge, Z. Giuseppe, and F. Piercarlo, J. Chem. Phys. **117**, 3120 (2002).
[18] J. H. Sinfelt, Bimetallic Catalysis, Discoveries Concepts and Applications, Wiley, New York 1983.
[19] W. Bouwen, F. Vanhoutte, and F. Despa, Chem. Phys. Lett. **314**, 227 (1999).

[20] E. Janssens, H. Tanaka, S. Neukermans, R. E. Silverans, and P. Lievens, New. J. Phys. **46**, 1 (2003).
[21] D. W. Yuan, Y. Wang, and Z. Zeng, J. Chem. Phys. **122**, 114310 (2005).
[22] H. Tanaka, S. Neukermans, and F. Janssens, J. Chem. Phys. **119**, 7115 (2003).
[23] H. P. Mao, H. Y. Wang, and Z. H. Zhu, J. Phys. **55**, 4542 (2006).
[24] X. Li, B. Kiran, and L. S. Wang, J. Phys. Chem. A **109**, 4366 (2005).
[25] J. J. Guo, J. X. Yang, and D. Die, J. Mol. Struct. (Theochem.) **764**, 117 (2006).
[26] J. X. Yang, J. J. Guo, and D. Die, J. Comp. (Theoretical) Chem. **963**, 435 (2011).
[27] M. Habar, S. Ouannssser, and L. Stauffer, Sur. Sa. **5**, 352 (1996).
[28] S. C. Wang, J. D. Wrigley, and G. Ehrlich, J. Chem. Phys. **91**, 5087 (1989).
[29] T. Y. Fu, T. Tien, and T. Song, Sur. Sci. **421**, 157 (1999).
[30] A. Berko and F. Solymosi, Sur. Sci. **411**, 900 (1998).
[31] D. C. Seets, M. C. Wheeler, and C. B. Mullins, Chem. Phys. Lett. **266**, 431 (1997).
[32] F. S. Lai and B. C. Gates, Nano Lett. **1**, 583 (2001).
[33] J. Dupont, G. S. Fonseca, A. P. Umpierre, P. F. P. Fichtner, and S. R. Teixeira, J. Am. Chem. Soc. **124**, 4228 (2002).
[34] G. S. Fonseca, A. P. Umpierre, P. F. P. Fichtner, S. R. Teixeira, and J. Dupont, J. Chem. Eur. **9**, 3263 (2003).
[35] K. Hayek, H. Goller, S. Penner, G. Rupprechter, and C. Zimmermann, Catal. Lett. **92**, 1 (2004).
[36] A. Berko and F. Solymosi, Sur. Sci. **411**, 900 (1998).
[37] J. Tao, J. P. Perdew, V. N. Staroverov, and G. E. Scuseria, Phys. Rev. Lett. **91**, 146401 (2003).
[38] M. J. Frisch, G. W. Trucks, H. B. Schlegel, G. E. Scuseria, M. A. Robb, J. R. Cheeseman, J. A. Montgomery, Jr., T. Vreven, K. N. Kudin, J. C. Burant, J. M. Millam, S. S. Iyengar, J. Tomasi, V. Barone, B. Mennucci, M. Cossi, G. Scalmani, N. Rega, G. A. Petersson, H. Nakatsuji, M. Hada, M. Ehara, K. Toyota, R. Fukuda, J. Hasegawa, M. Ishida, T. Nakajima, Y. Honda, O. Kitao, H. Nakai, M. Klene, X. Li, J. E. Knox, H. P. Hratchian, J. B. Cross, V. Bakken, C. Adamo, J. Jaramillo, R. Gomperts, R. E. Stratmann, O. Yazyev, A. J. Austin, R. Cammi, C. Pomelli, J. Ochterski, P. Y. Ayala, K. Morokuma, G. A. Voth, P. Salvador, J. J. Dannenberg, V. G. Zakrzewski, S. Dapprich, A. D. Daniels, M. C. Strain, O. Farkas, D. K. Malick, A. D. Rabuck, K. Raghavachari, J. B. Foresman, J. V. Ortiz, Q. Cui, A. G. Baboul, S. Clifford, J. Cioslowski, B. B. Stefanov, G. Liu, A. Liashenko, P. Piskorz, I. Komaromi, R. L. Martin, D. J. Fox, T. Keith, M. A. Al-Laham, C. Y. Peng, A. Nanayakkara, M. Challacombe, P. M. W. Gill, B. G. Johnson, W. Chen, M. W. Wong, C. Gonzalez, and J. A. Pople, GAUSSIAN 03 (Revision E.01), Gaussian, Inc., Wallingford, CT 2004.
[39] W. J. Stevens, M. Krauss, H. Basch, and P. G. Jasien, Can. J. Chem. **70**, 612 (1992).
[40] J. L. Jules and J. R. Lombardi, J. Phys. Chem. A **107**, 1268 (2003).
[41] K. P. Huber and G. Herzberg, Constants of Diatomic Molecules, Molecular Spectra and Molecular structure, vol. 4, Van Nostrand Reinhold, New York 1979.
[42] A. R. Miedema and K. A. Gingerich, At. Mol. Phys, J. Phys. B **12**, 2081 (1979).
[43] J. L. Jules and J. R. Lombardi, J. Phys. Chem. A **107**, 1268 (2003).
[44] J. G Du and X. Yuan, J. Phys. Chem. A **114**, 12825 (2010).
[45] G. Balducci, A. Ciccioli, and G. Gigli, J. Chem. Phys. **121**, 7748 (2004).
[46] A. Nijamudheen and A. Datta, J. Mol. Struct. (Theochem) **945**, 93 (2010).
[47] B. Assadollahzadeh and P. Schwerdtfeger, J. Chem. Phys. **131**, 064306 (2009).
[48] H. M. Lee, M. Ge, B. R. Sahu, P. Tarakeshwar, and K. S. Kim, J. Phys. Chem. B **107**, 9994 (2003).
[49] H. Hakkinen and U. Landman, Phys. Rev. B **62**, 2287 (2000).
[50] A. B. Sannigrahi, P. K. Nandi, and P. R. Schleyer, J. Am. Chem. Soc. **116**, 7225 (1994).